Phosphorylated Claudin-16 interacts with Trpv5 and regulates transcellular calcium transport in the kidney

Jianghui Hou[1], Vijay Renigunta[2], Mingzhu Nie[3], Abby Sunq[1], Nina Himmerkus[4], Catarina Quintanova[4], Markus Bleich[4], Aparna Renigunta[5], Matthias Tilmann Florian Wolf[3]

[1]Department of Internal Medicine – Renal Division, Washington University St Louis, St Louis, Missouri, USA; Department of Neurophysiology, Institute of Physiology and Pathophysiology, Philipps-University Marburg, 35037 Marburg, Germany; [3]Department of Pediatrics, Pediatric Nephrology, University of Texas Southwestern Medical Center, Dallas, Texas, USA; [4]Department of Physiology, University of Kiel, Kiel, Germany; [5]University Children's Hospital, University of Marburg, Marburg, Germany.

*Corresponding author:
Jianghui Hou, PhD.
Washington University St Louis
660 South Euclid Avenue
St Louis, MO 63110
USA
Email: jhou@wustl.edu

www.pnas.org/cgi/doi/10.1073/pnas.1902042116

SI Figure

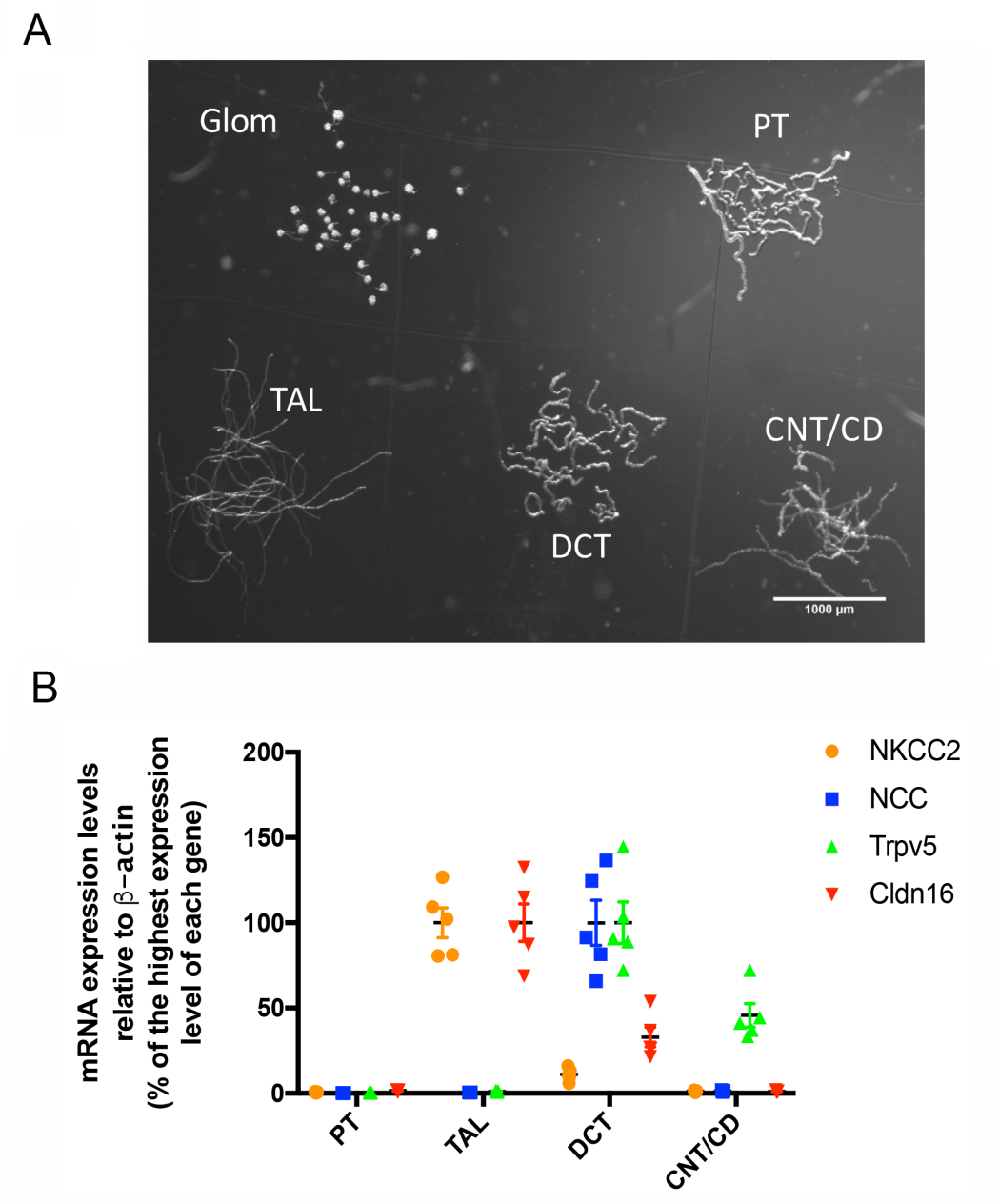

Figure S1. Claudin-16 gene expression in the mouse kidney. (A) Panel of images showing microdissected renal tubules from the mouse kidney. Microdissection criterion: (i) PCT, DCT, and TAL joined at glomerulus/macula densa were dissected out; (ii) glomerulus and PCT were separated from macula densa; (iii) PCT was separated from glomerulus and DCT was separated from TAL at the junction of macula densa; (iv) CNT/CD was separated from DCT according to morphological differences. (B) Claudin-16 mRNA levels relative to β-actin mRNA levels in microdissected nephron segments. N=5 animals, ~200 microdissected tubules for each nephron segment from each animal. NKCC2, NCC, and Trpv5 mRNA levels were also measured and shown here. Note that the DCT segment includes macula densa, which might explain the residual expression of NKCC2.

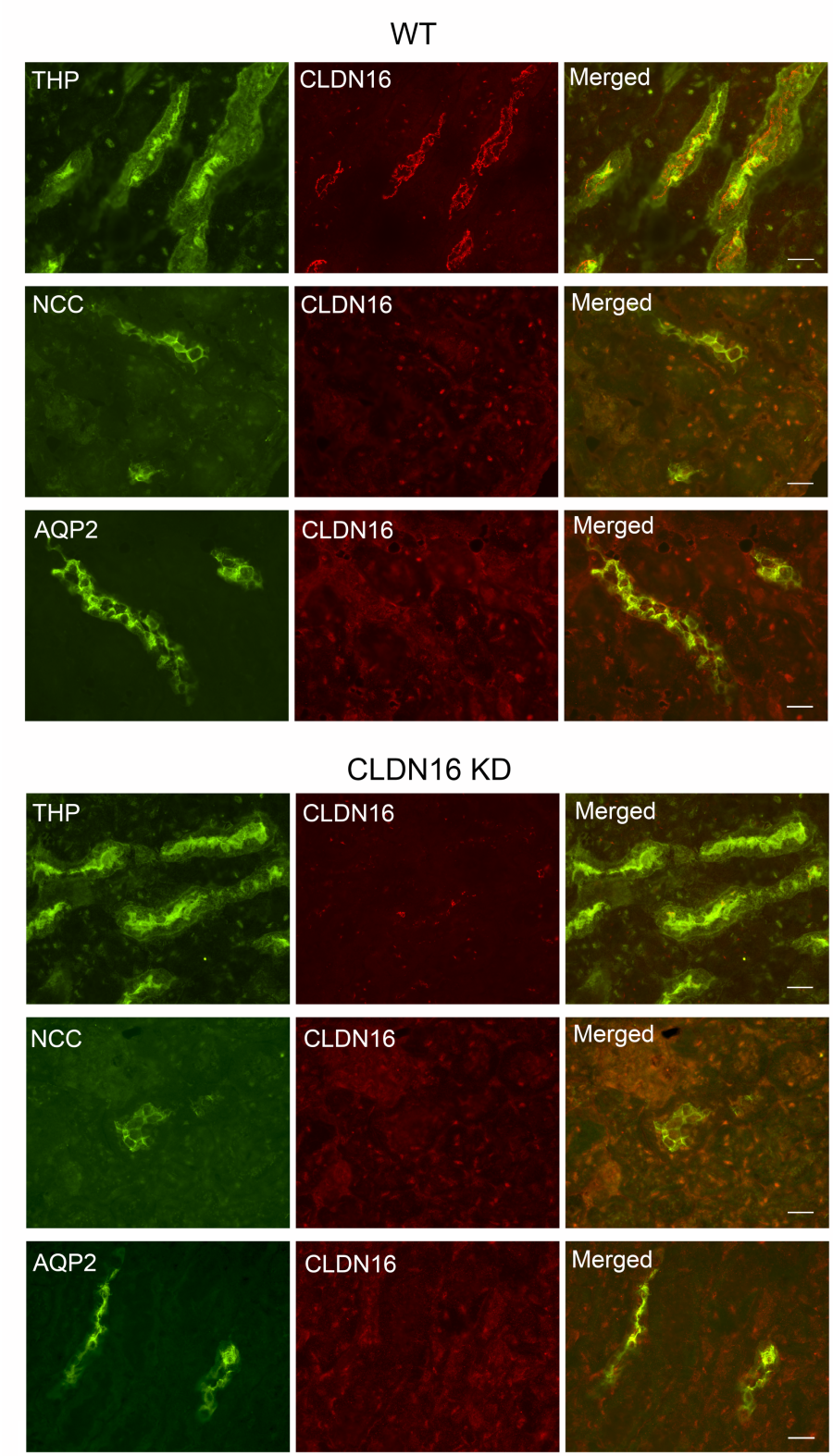

Figure S2. Claudin-16 protein localization in the mouse kidney. Dual immunofluorescent staining of claudin-16 protein (CLDN16) with a TAL marker (THP), with a DCT marker (NCC), and with a CNT/CD marker (AQP2) in WT and CLDN16 KD mouse kidneys. Scale bar: 20 μm.

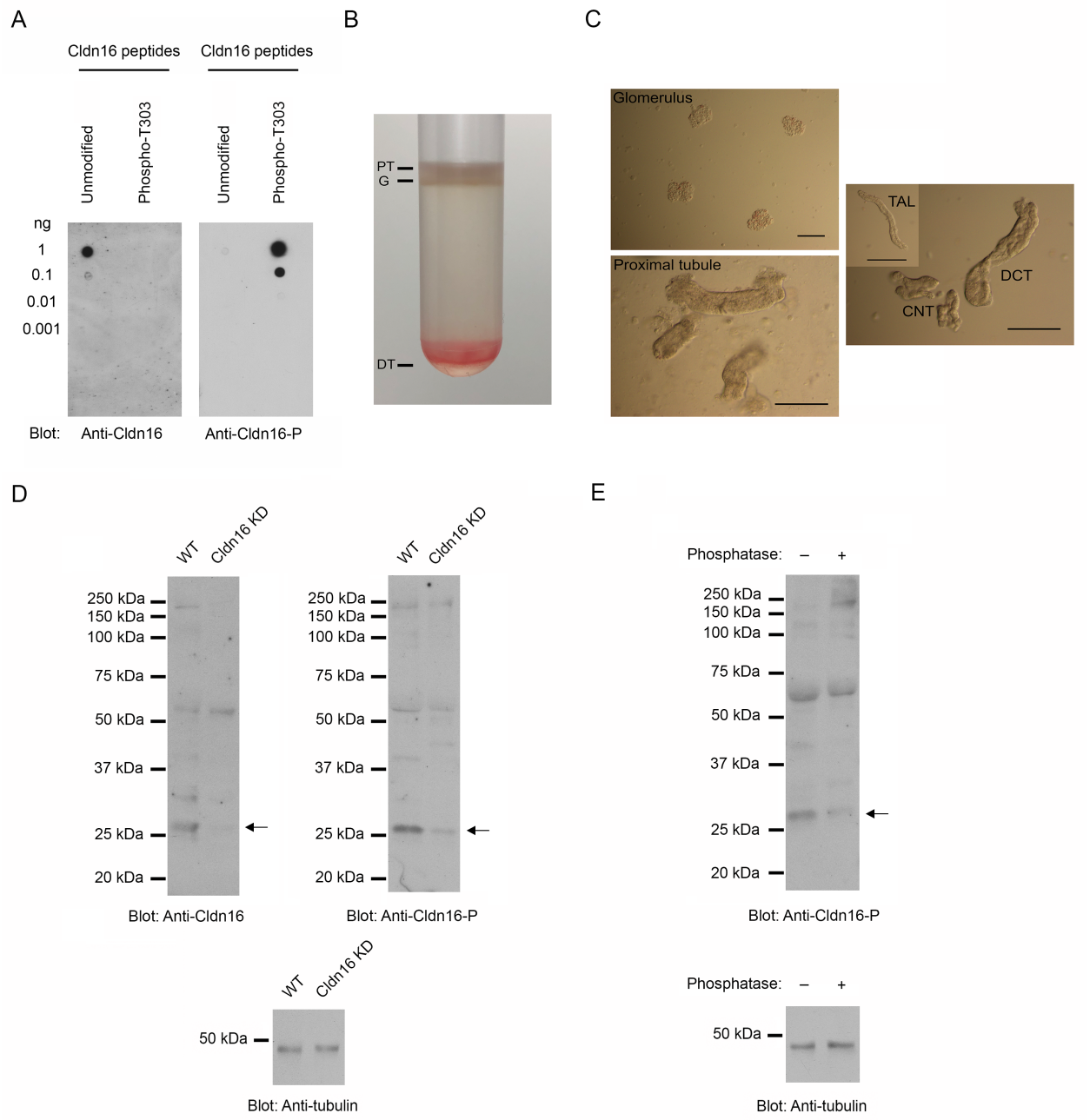

Figure S3. Characterization of claudin-16 Phospho-T303 antibody. (A) The binding assay of claudin-16 antibodies to phosphorylated or nonphosphorylated peptide. Peptides were loaded onto nitrocellulose membrane at different concentrations and blotted against a regular claudin-16 antibody or a phosphorylated claudin-16 antibody. (B) Percoll gradient was used to separate the distal tubules from the proximal tubules and the glomeruli. (C) Microscopic graphs showing the isolated renal tubular segments. (D) Membrane lysates of the purified distal tubules from WT and CLDN16 KD mouse kidneys were blotted against the regular claudin-16 antibody and the phosphorylated claudin-16 antibody. (E) Membrane lysates of the purified distal tubules from the WT mouse kidney were treated with λ-phosphatase and blotted against the phosphorylated claudin-16 antibody. Arrow indicates the claudin-16 band and anti-tubulin antibody was used for loading control in D and E.

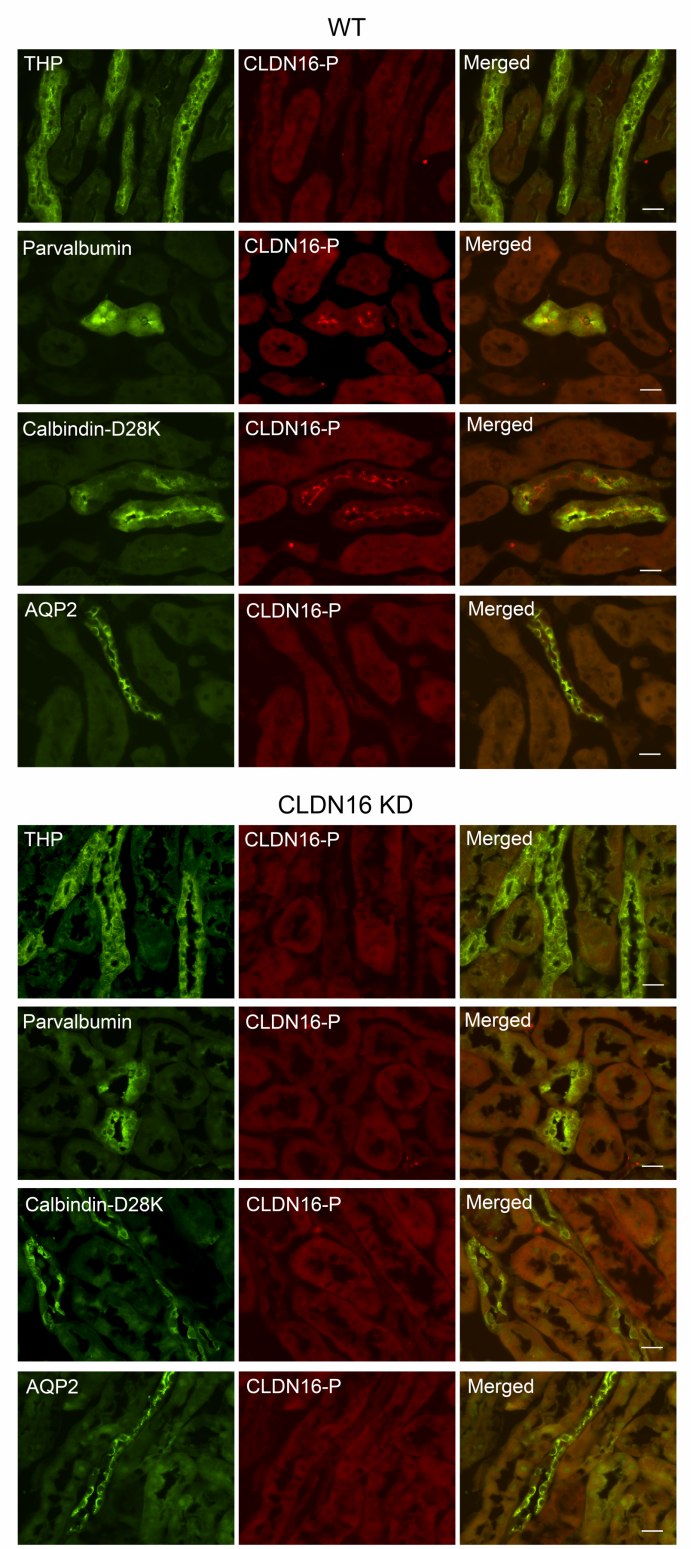

Figure S4. Phosphorylated claudin-16 protein localization in the mouse kidney. Dual immunofluorescent staining of phosphorylated claudin-16 protein (CLDN16-P) with a TAL marker (THP), with a DCT1 marker (Parvalbumin), with a DCT2 marker (Calbindin-D28K), and with a CNT/CD marker (AQP2) in WT and CLDN16 KD mouse kidneys. Scale bar: 20 μm.

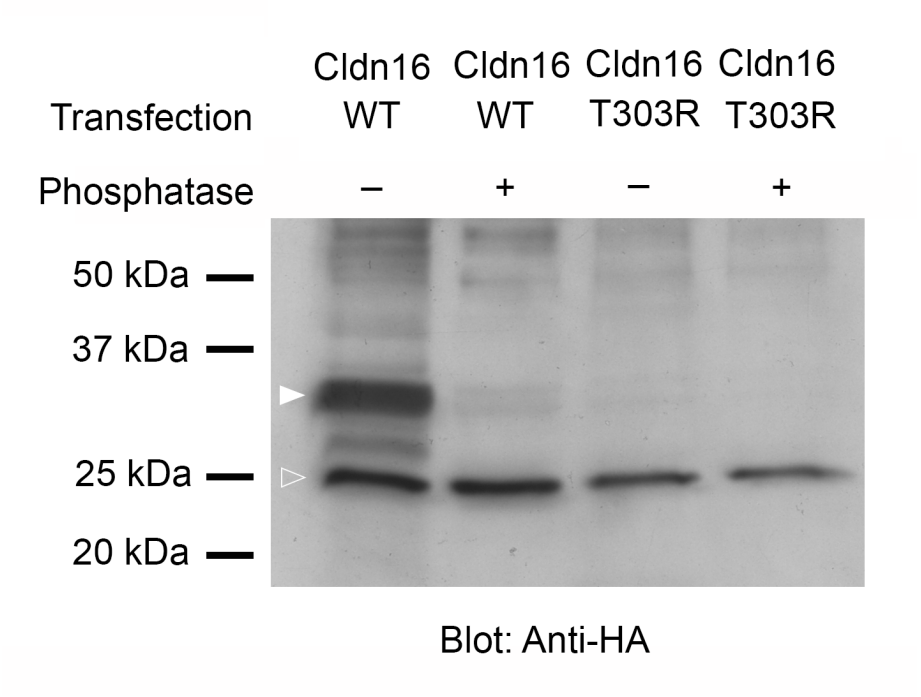

Figure S5. Claudin-16 phosphorylation in cultured MDCT cells. Immunoblot of N-terminally HA-tagged claudin-16 after Phos-tag SDS PAGE reveals the presence of a major phosphorylated band (filled arrowhead, 30 kDa) retarded by the Phos-tag ligand in the PAGE gel. Treatment with λ-phosphatase reduced the upper phosphorylated band to the size of unphosphorylated claudin-16 (open arrowhead, 25 kDa). Note that the phosphorylated band is absent in the T303R mutant. Also note that 30 kDa is not the true molecular weight of phosphorylated claudin-16.

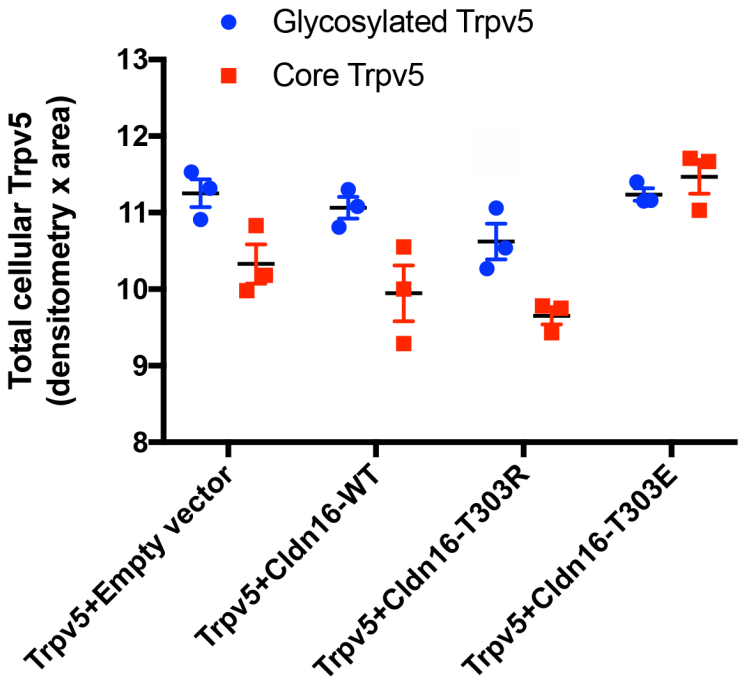

Figure S6. Total cellular Trpv5 protein abundance levels. Statistical graph showing trpv5 abundance levels in cells expressing Trpv5 with claudin-16 variant proteins, including wildtype (WT), dephosphorylated (T303R) and phosphomimetic (T303E) claudin-16. Trpv5 proteins migrate as two separate bands on PAGE gel: 82 kDa core protein (white arrow) and 92 kDa glycosylated protein (black arrow) (**Figure 4**).

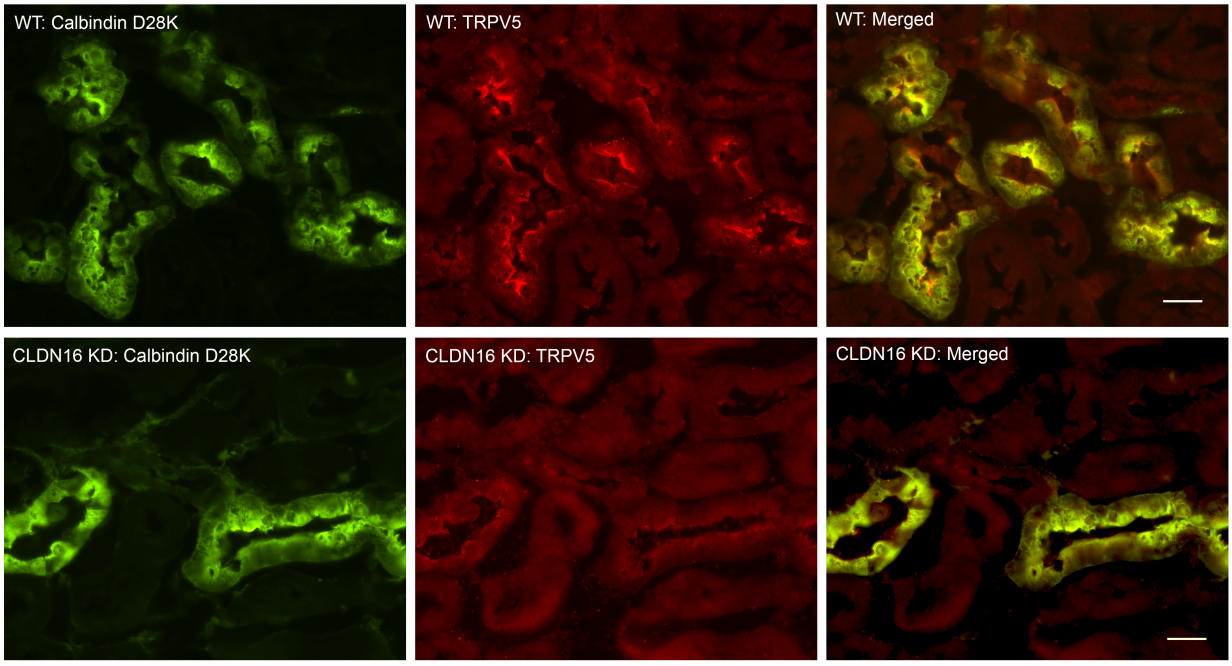

Figure S7. Confirming Trpv5 localization change in claudin-16 KD mouse kidney with a second Trpv5 antibody. Dual immunofluorescent immunostaining of Trpv5 with the DCT2 marker (Calbindin-D28K) on the kidney sections from WT and claudin-16 KD mice. The goat anti-Trpv5 from Abcam was used in this experiment. Scale bar: 20 μm.

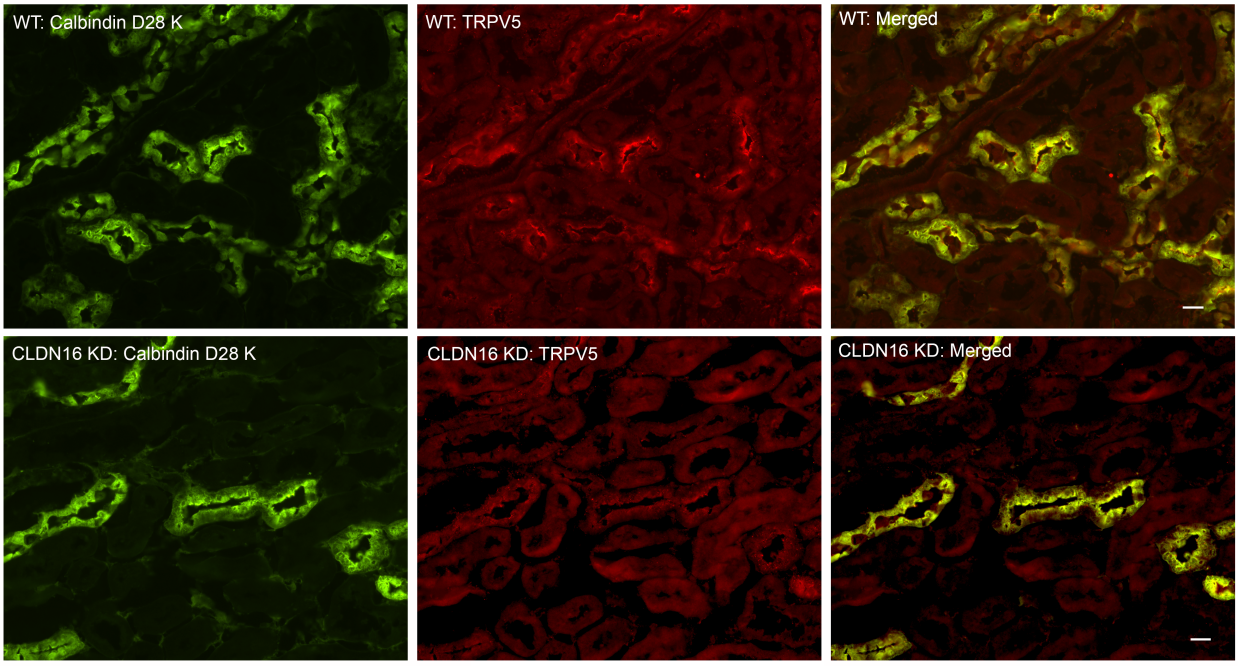

Figure S8. Low-magnification images of Trpv5 localization in claudin-16 KD mouse kidney. Dual immunofluorescent immunostaining of Trpv5 with the DCT2 marker (Calbindin-D28K) on the kidney sections from WT and claudin-16 KD mice. The goat anti-Trpv5 from Abcam was used in this experiment. Scale bar: 20 μm.

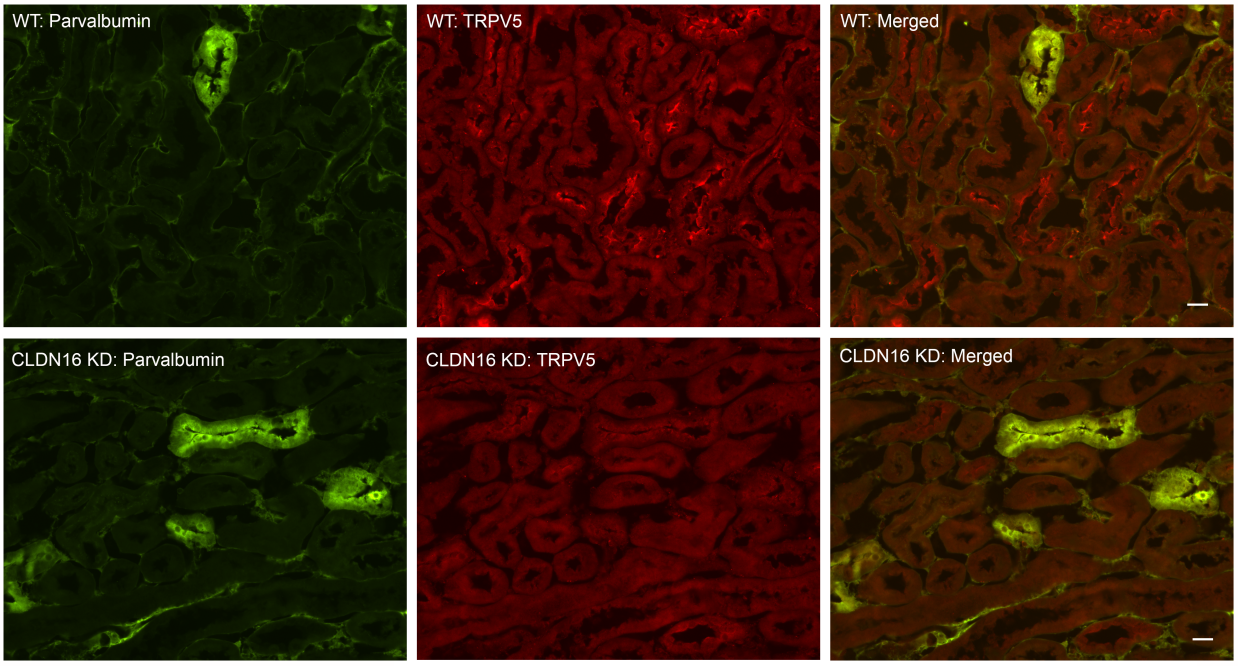

Figure S9. Trpv5 localization in the DCT1 tubules from WT and claudin-16 KD mouse kidneys. Dual immunofluorescent immunostaining of Trpv5 with the DCT1 marker (Parvalbumin) on the kidney sections from WT and claudin-16 KD mice. The goat anti-Trpv5 from Abcam was used in this experiment. Scale bar: 20 μm.

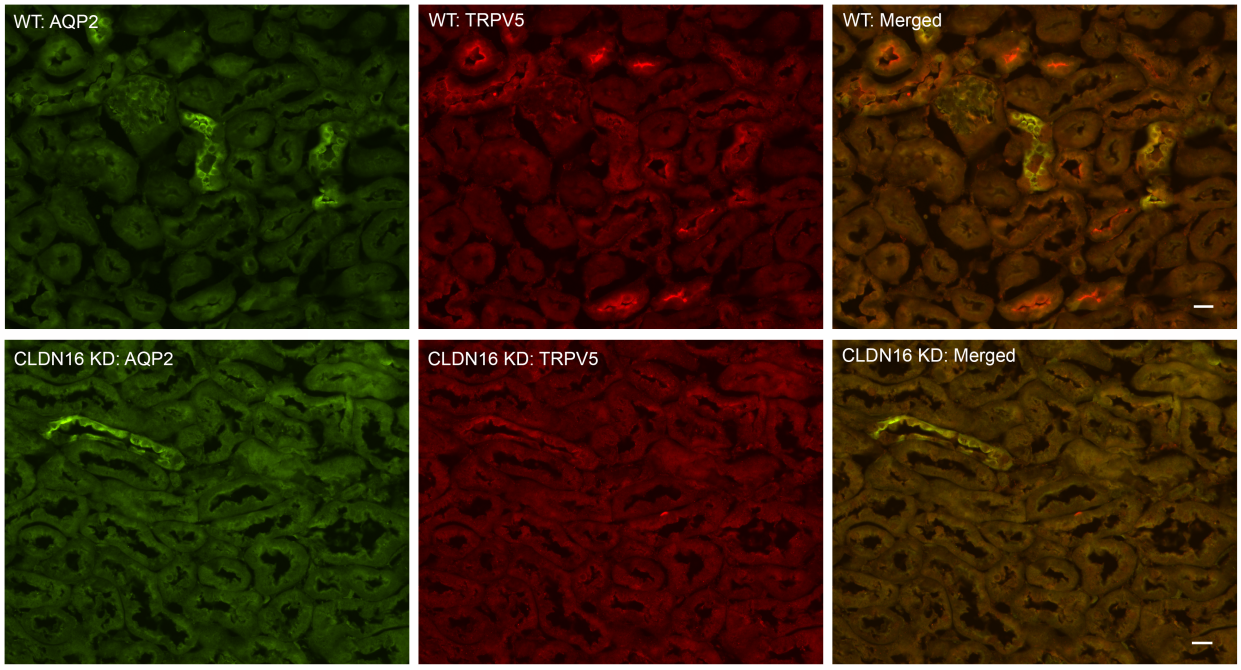

Figure S10. Trpv5 localization in the CNT tubules from WT and claudin-16 KD mouse kidneys. Dual immunofluorescent immunostaining of Trpv5 with the CNT marker (Aqp2) on the kidney sections from WT and claudin-16 KD mice. The goat anti-Trpv5 from Abcam was used in this experiment. Scale bar: 20 μm.

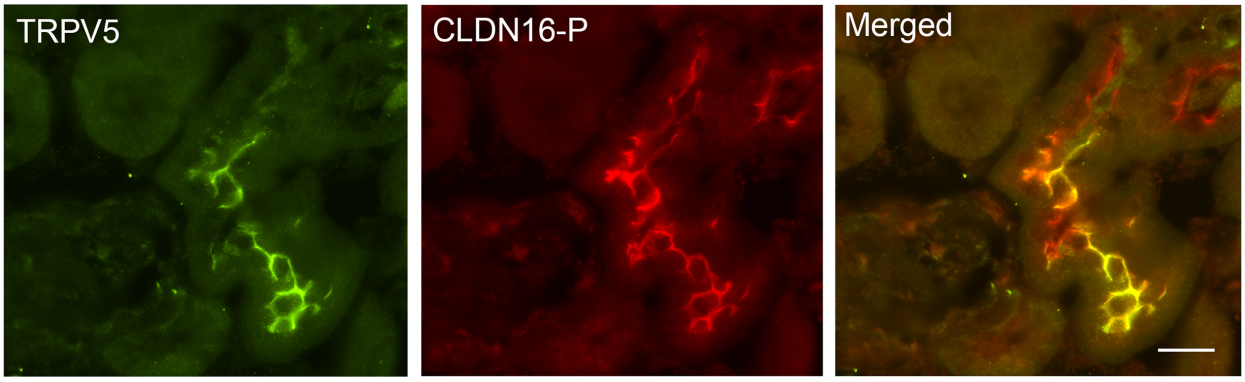

Figure S11. Colocalization of phosphorylated claudin-16 with Trpv5 on kidney sections. Immunostaining of WT mouse kidney sections showing colocalization of Trpv5 with phosphorylated claudin-16 (detected with anti-CLDN16-P antibody) in the distal tubules. Scale bar: 20 μm.

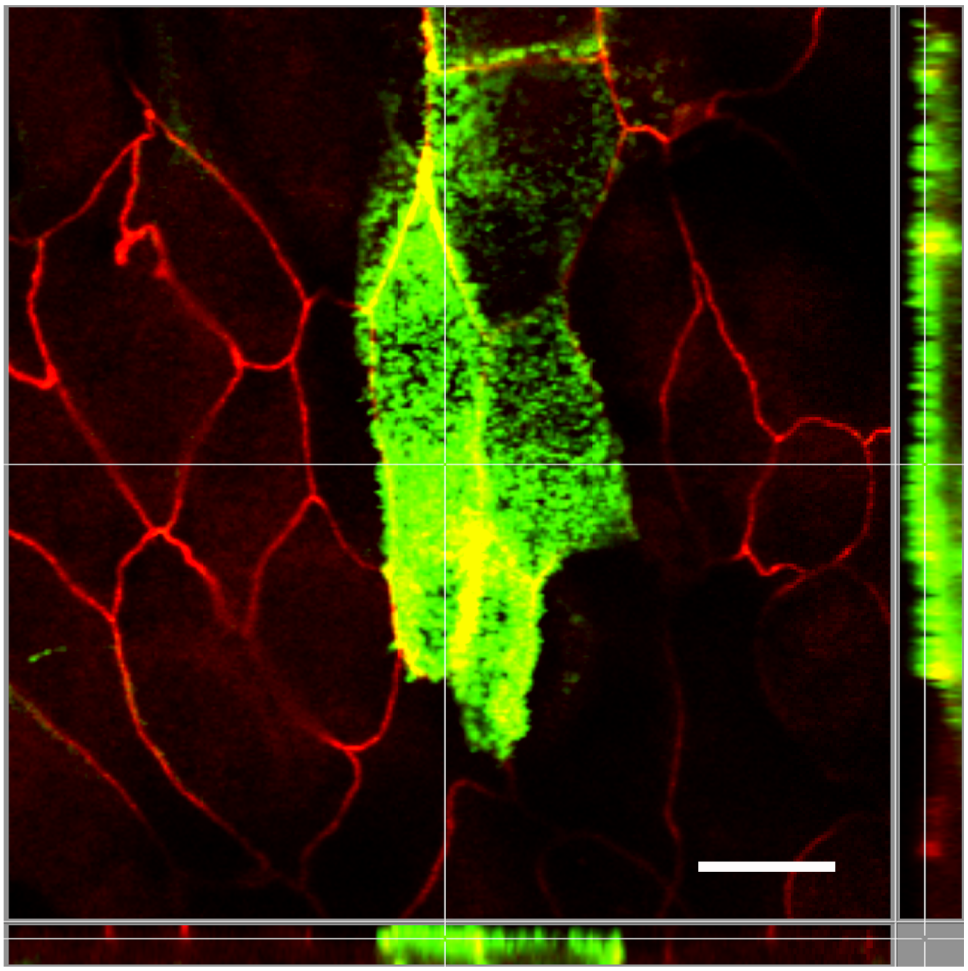

Figure S12. Apical membrane localization of phosphomimetic claudin-16 in LLC-PK1 cells. 3D rendered confocal images showing the apical membrane localization of phosphomimetic claudin-16 (green) in transfected LLC-PK1 cells. The TJ was labeled with an antibody against ZO-1 (red). Scale bar: 10 μm.

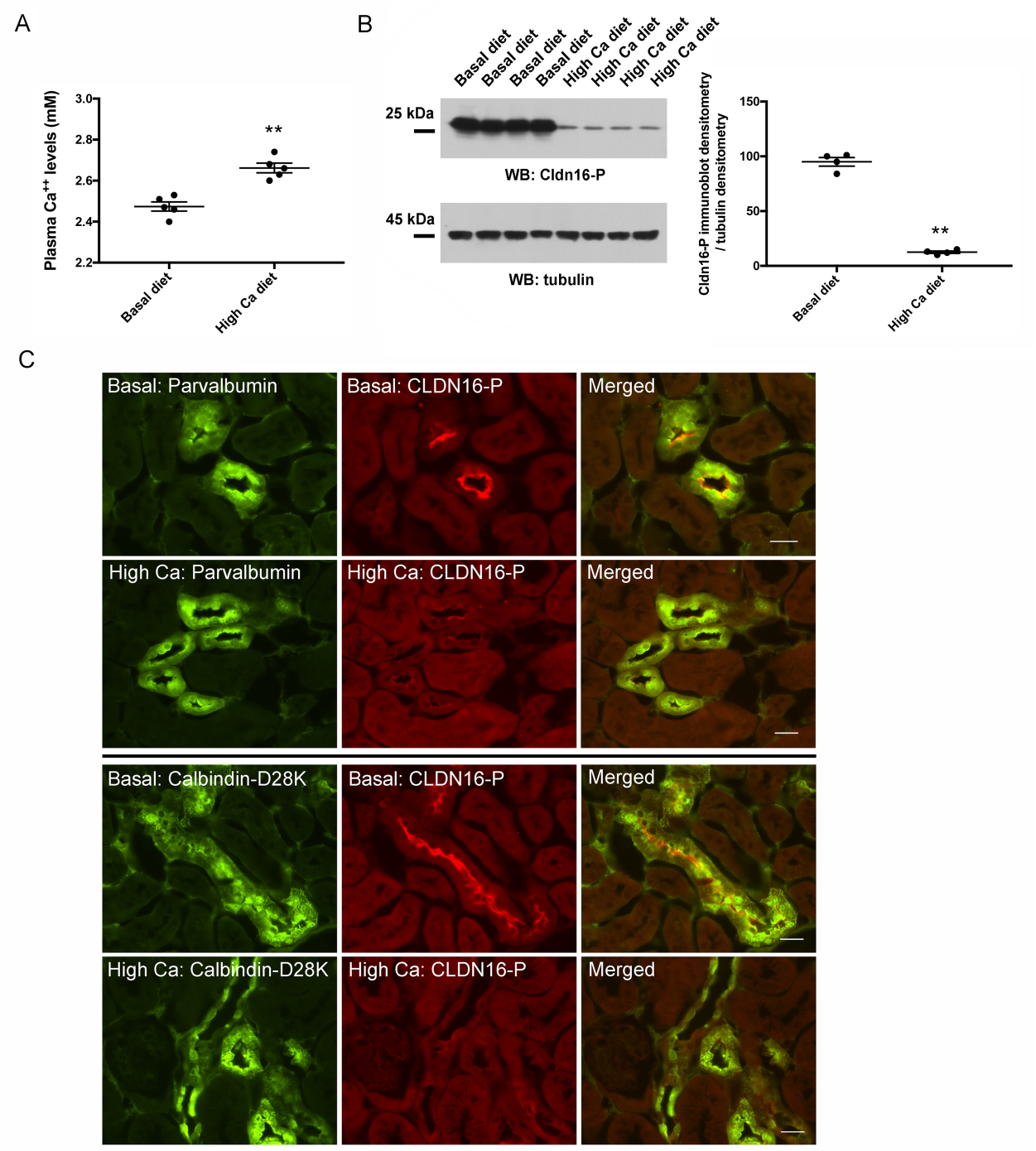

Figure S13. Claudin-16 phosphorylation levels in high Ca^{++} diet treated mice. (A) The plasma Ca^{++} levels in mice receiving dietary Ca^{++} variations. (B) Freshly isolated mouse distal tubular cells were lysed in Laemmli buffer and immunoblotted against anti-CLDN16-P antibody to reveal claudin-16 phosphorylation levels. Anti-tubulin antibody was used for loading control. **, $p<0.01$, n=4 animals. (C) Dual immunofluorescent staining of phosphorylated claudin-16 protein (CLDN16-P) with the DCT markers (Parvalbumin and Calbindin-D28K). Scale bar: 20 μm.